

See discussions, stats, and author profiles for this publication at: <https://www.researchgate.net/publication/350311007>

Quantum Track Reconstruction Algorithms for non-HEP applications

Conference Paper · February 2021

DOI: 10.22323/1.390.0983

CITATIONS

0

READS

3

10 authors, including:



Cenk Tüysüz

Middle East Technical University

8 PUBLICATIONS 58 CITATIONS

[SEE PROFILE](#)



Federico Carminati

Transmutex

385 PUBLICATIONS 17,888 CITATIONS

[SEE PROFILE](#)



Fabio Fracas

University of Padova

9 PUBLICATIONS 4 CITATIONS

[SEE PROFILE](#)

Some of the authors of this publication are also working on these related projects:



ALICE CAF [View project](#)



ALICE Interactive Grid [View project](#)

Quantum Track Reconstruction Algorithms for non-HEP applications

Kristiane Novotny^{*1}, Cenk Tüysüz², Carla Rieger³, Daniel Dobos^{1,4}, Karolos Potamianos^{1,5}, Bilge Demirköz², Federico Carminati⁶, Sofia Vallecorsa⁶, Jean-Roch Vlimant⁷, Fabio Fracas^{6,8}

¹gluonNet, ²METU, Ankara, ³ETH Zürich, ⁴University of Lancaster, ⁵University of Oxford,

⁶CERN openlab, ⁷Caltech, ⁸University of Padua

E-mail: kristiane@gluonnet.org

The expected increase in simultaneous collisions creates a challenge for accurate particle track reconstruction in High Luminosity LHC experiments. Similar challenges can be seen in non-HEP trajectory reconstruction use-cases, where tracking and track evaluation algorithms are used. High occupancy, track density, complexity and fast growth therefore exponentially increase the demand of algorithms in terms of time, memory and computing resources. While traditionally Kalman filter (or even simpler algorithms) are used, they are expected to scale worse than quadratic and thus strongly increasing the total processing time. Graph Neural Networks (GNN) are currently explored for HEP, but also non HEP trajectory reconstruction applications. Quantum Computers with their feature of evaluating a very large number of states simultaneously are therefore good candidates for such complex searches in large parameter and graph spaces. In this paper we present our work on implementing a quantum-based graph tracking machine learning algorithm to evaluate Traffic collision avoidance system (TCAS) probabilities of commercial flights.

*The 40th International Conference on High Energy Physics (ICHEP2020)
28 July-06 August, 2020
Prague, Czech Republic*

*Speaker.

1. Introduction

With the start of the data taking period of the High-Luminosity LHC [1] and even with building a potential Future Circular Collider, the amount of collisions and with it the amount of data is expected to increase significantly. Current machine learning techniques are able to cope with the existing data but are expected to outperform soon. Similar problems appear in the aviation industry with the increased usage of drones and the mandatory use of ADS-B [2]. Novel techniques such as quantum computing are considered as potential candidates to overcome these problems.

A collaboration has been formed between gluONNet, CERN openlab, the Middle Technical East University of Ankara as well as researchers from the University of Oxford and Caltech to explore possible applications of quantum computing algorithms to particle track reconstruction problems and reconstructing airplane routes due to striking similarities between them. One of these similarities are the detector hit and the broadcasted information as both include time and position information. Airplanes correspond to particles in this comparison and the event Id then corresponds to the aircraft's unique identifier. In this study, the track reconstruction of airplanes has the major aim of understanding triggers leading to deviations of the flown path compared to the optimal route. In a future step, this could then be applied for optimizing airport capacities, for understanding environmental aspects as well as for improving predictions of potential collisions by the Traffic Collision Avoidance System (TCAS). This system warns the aviator of a potential collision in a given area and requests one aircraft to ascend, while the other is requested to descend. The area of interest is a cylinder with a height of about one kilometre and a diameter about 55 kilometres. Then the actual size changes depending on the aircraft's height. The TCAS has become decisive for potential collisions after two aircrafts collided due to an erroneous suggestion by an air traffic controller, while the TCAS had given the correct advice.

For our study, we consider first the physics case and then we derive from that the implications for the aviation case. Although the focus will be on the particle physics case, it still remains applicable to the aviation case. In particle physics, particles collide and produce hits, which are signals recorded by the detector. Algorithms then associate a hit to a particle, whereas other algorithms that are expected to outperform reconstruct the particle's trajectory. A dedicated challenge has been initiated by CERN on Kaggle to develop new algorithms for the future based on a data set that is now used as a set to benchmark existing code [3, 4].

2. The data sets

The Kaggle data set contains 10k events and is publicly available [3, 4]. One hundred events of the available data set are used due to the long processing time in the order of one week of the quantum computing code. This corresponds to 1% of the available data. Events covering the barrel region of the detector have been selected due to the closeness to the origin of the collision point as well as due to a reduction of the amount of data. Following Hep-TrkX [5], the cuts on pseudorapidity $\eta \in [-5, 5]$, the angle ϕ of the transverse plane and beam direction z have been applied. The precise values are shown in Tab.1. In addition, the transverse plane is divided into 8 slices. The graph matrices are constructed by using Hep-TrkX's pre-processing [5]. These matrices contain the spatial information, which are then fed to the Quantum Graph Neural Net.

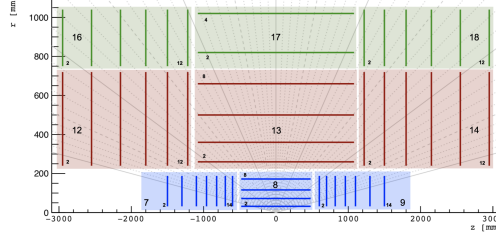


Figure 1: Detector layout of the TrackML challenge. The barrel region corresponding to horizontal layers in this drawing covers parts of the volume with the IDs 8, 13, and 17 has been taken into account [3, 4].

Parameter	Selection
$ p_T $	$> 1 \text{ GeV}$
$\Delta\phi$	< 0.0006
z_0	$< 100 \text{ mm}$
η	$[-5, 5]$

Table 1: Selections applied to TrackML dataset for preprocessing.

3. Hybrid Graph Neural Networks

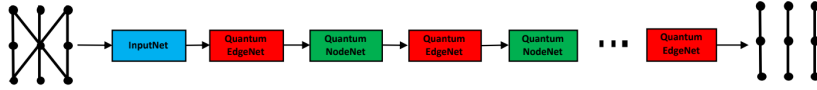


Figure 2: Structure of iterative application of the Quantum Node Network and Quantum Edge Network.

The Quantum Graph Neural Network (QGNN) is a hybrid version, i.e., consisting of classical parts and quantum circuits. Its overall architecture is based on the work of the Hep-TrkX project [5]. Their classical model uses an Input Network followed by an iterative application of an edge network and a node network. The network pipeline is shown in Fig.2, in which the graphs are depicted as black lines connecting dots and the Input Network is displayed in blue, followed by the iterative application of the Edge and Node networks depicted in red and green. This architecture is modified by implementing quantum circuits as an underlying model for edge and node networks, which is why the terms quantum edge network and quantum node networks are used. The overall network pipeline is encoded using Tensorflow [6] as well as PennyLane [7] connecting the quantum circuits with the classical networks. In case of the quantum circuits, two shallow and low width architectures have been chosen as they can be executed on Noisy Intermediate-Scale Quantum devices. The first architecture of the quantum circuits has been a Tensor Tree network (TTN) and the second architecture has been improved to a multi-scale entanglement renormalization ansatz (MERA) [8] network.

Edge network and Node network serve different purposes, which are examined in the following. The circuits are created for each network differently because they differ in the number of qubits.

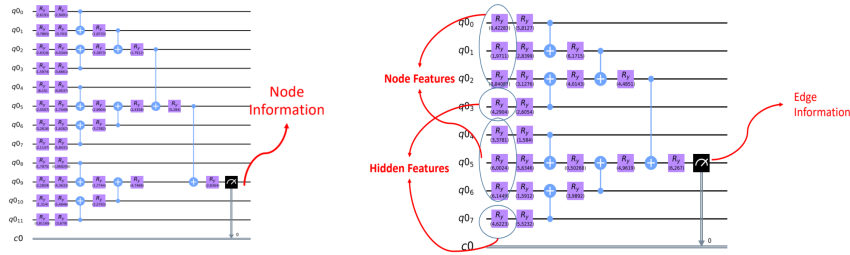


Figure 3: Quantum Node Network (left) and Quantum Edge Network (right) are composed of Tensor Tree Networks (TTN). The underlying TTNs differ in the amount of qubits. 6 qubits are used to cover two sets of three spatial coordinates corresponding to two edges. The hidden features correspond to classical neural network layers. The obtained output of the Quantum Edge Network serves as input for the Quantum Node Network. Numerical values are example values.

3.1 Edge Network

After having passed the input network that maps the dimension of the graph matrices to the dimension of the edges, the data are fed into the first Quantum Edge network, which is displayed on the right hand side in Fig. 3. The edge network contains 8 qubits, in which two hits are taken into account. Each spatial coordinate of one hit corresponds to one qubit and there is one extra qubit to increase the size of the network’s hidden dimension. The additional qubit corresponds to hidden layers in a classical neural network. Each qubit is rotated around an angle θ on the y axis using R_y rotation gates. The data input corresponds to the angle and is therefore mapped to an interval $[0, \pi]$ due to the existence of a cosine function in the gate. Half of the cosine’s period is conserved in order to avoid unwanted overlap.

3.2 Node network

The node network shown on the left hand side in Fig. 3 has a similar structure as the Edge network. If the size of the hidden dimension is one in the node network, there are four more qubits than in the edge network. In total, the information of three nodes are taken into account. Two of these three nodes correspond to neighbouring nodes around a centred node.

4. Training and results

The training set contains 1400 subgraphs and has been validated by 200 randomly selected subgraphs. The order of the validation sets are shuffled, whereas the order in the validation set has been kept. The edge probability is defined as average of the measurement outcomes. Afterwards, the uncertainty is calculated based on the ground truth. Tensorflow’s ADAM optimiser [9] is used as an optimiser with learning rates of 0.03 in case of the architecture displayed in orange in Fig. 4 and 0.005 in case of the new version, displayed in blue in Fig. 4. The architectures differ in the amount of measurement. The new version takes only one measurement, contrary to the architecture of the network that produces the orange band. The underlying model resulting in the blue curve differs between the one that produces the orange curve by the fact that there is only one direct measurement taken. Algorithms used for the gradient calculation require longer processing times

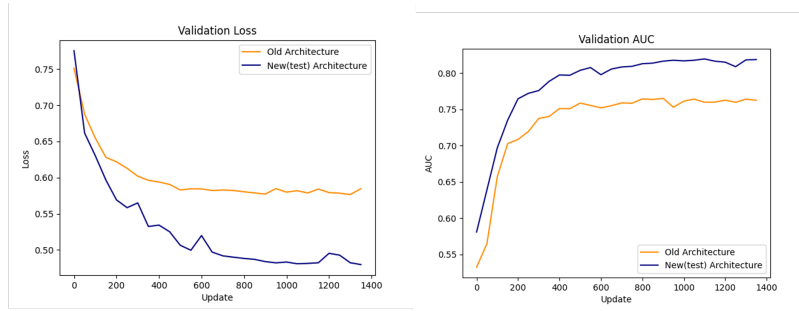


Figure 4: Comparison between different architectures. The loss decreases, whereas the accuracy increases in case of the new architecture with a learning rate of 0.005. Only a single measurement has been performed. The investigation has been done for one single epoch.

for obtaining gradients of the quantum circuits, which requires reiterations of those circuits with different parameters. Only simulations of quantum circuits have been used in this work due to the limited access to real quantum hardware. Tests to train the network have been performed using 4 qubits and circuits 6, 11, 14 and 15 of [10] as well as with 4 qubit versions of the Tensor Tree Network and MERA. These circuits have a high entanglement capability as well as not too many trainable parameters. As a result, the learning rate is small using 5 epochs. This is, however, not surprising as comparable classical graph neural networks suggest requiring at least 66 epochs for a sufficient Node classification and 96 epochs for a graph classification [11].

5. Conclusions and outlook

This work is an extension of our prior work [12]. It has been shown that quantum computing models are an intriguing possibility for applications in both particle physics and industry. Although these models are not yet competitive due to the limited access to real quantum computers, it might offer a good alternative for the future.

Next steps will include an increased number of qubits as well as optimization methods. GPUs decrease the processing time as well as working with parameterized quantum circuits.

It is now planned to deploy this to the aviation case. We already have started to look into the ADS-B data set. ADS-B is a broadcasting system using satellites and has a world-wide coverage [2]. Aircrafts broadcast their information to satellites, which then transmit the signal to ground stations. This information contains the aircraft’s position in degrees of Longitude and Latitude in the WGS-84 format, as well as the projected height to the earth’s ellipsoid and the aircraft’s unique transponder identification number. Any further information is not mandatory for transmission and therefore not always available [13]. The studied data set has a size of 500 GB and covers commercial aircraft data of the CAT 21 for April 2019. It has been kindly provided by Aireon [14] and the Irish Aviation Authority [15].

6. Acknowledgments

K.N., K.P. and D.D. thank Peter Griffiths and Jeff Ashbolt for fruitful discussions. Part of this work was conducted at "iBanks", the AI GPU cluster at Caltech. We acknowledge

POS (ICHEP2020) 983

NVIDIA, SuperMicro and the Kavli Foundation for their support of "*iBanks*". This work was partially supported by Turkish Atomic Energy Authority (TAEK) (Grant No: 2017TAEKCERN-A5.H6.F2.15).

References

- [1] G. Apollinari, et al. "High Luminosity Large Hadron Collider HL-LHC," CERN Yellow Report **2015-005**, 1-19 (2017) [arXiv:1705.08830 [physics.acc-ph]].
- [2] ADS-B Exchange <https://www.adsbexchange.com/data/>.
- [3] <https://www.kaggle.com/c/trackml-particle-identification/data>
- [4] S. Amrouche, L. Basara, P. Calafiura, V. Estrade, S. Farrell, D. R. Ferreira, L. Finnie, N. Finnie, C. Germain and V. V. Gligorov, *et al.* "The Tracking Machine Learning challenge : Accuracy phase," doi:10.1007/978-3-030-29135-8_9 [arXiv:1904.06778 [hep-ex]].
- [5] S. Farrell, et al. "Novel Deep Learning Methods for Track Reconstruction," [arXiv:1810.06111 [hep-ex]].
- [6] M. Abadi, et al. "TensorFlow: Large-Scale Machine Learning on Heterogeneous Systems," <https://www.tensorflow.org/>, (2015).
- [7] E. Grant et al., "PennyLane: Automatic Differentiation of Hybrid Quantum-Classical Computations," [arXiv:1811.04968 [quant-ph]].
- [8] Grant et al., "Hierarchical quantum classifiers," *npj Quantum Information*, vol4, no.1, pp.17–19, 2018. 10.1038/s41534-018-0116-9
- [9] Diederik P. Kingma and Jimmy Ba "Adam: A Method for Stochastic Optimization," [arXiv:1412.6980 [cs]]
- [10] Sim et al., "Expressibility and Entangling Capability of Parameterized Quantum Circuits for Hybrid Quantum-Classical Algorithms," *Advanced Quantum Technologies* vol.2, no.12, <http://dx.doi.org/10.1002/qute.201900070>
- [11] V. P. Dwivedi et al., "Benchmarking Graph Neural Networks," [arXiv:2003.00982 [cs.LG]].
- [12] C. Tüysüz, F. Carminati, B. Demirköz, D. Dobos, F. Fracas, K. Novotny, K. Potamianos, S. Vallecorsa and J. R. Vlimant, "A Quantum Graph Neural Network Approach to Particle Track Reconstruction," [arXiv:2007.06868 [quant-ph]].
- [13] EUROCONTROL Specification for Surveillance Data Exchange ASTERIX Part 12 Category 21 ADS-B Target Reports, EUROCONTROL-SPEC-0149-12, <https://www.eurocontrol.int/publication/cat021-eurocontrol-specification-surveillance-data-exchange-asterix-part-12-category-21>
- [14] Aireon-SPACE-BASED ADS-B <https://aireon.com/>.
- [15] Irish Aviation Authority. <https://www.iaa.ie/>.